CBN-07-11
August, 2007

Emittance Growth Due to Space Charge Forces in an Electron Bunch Compressor

Richard Talman, Cornell Laboratory of
Elementary-Particle Physics
and
Nikolay Malitsky, Brookhaven National Laboratory

Abstract. Using the UAL (Unified Accelerator Libraries) string space charge formulation,[**1**][**2**][**3**] this paper simulates electron bunch compression results obtained at CTF-II, the CERN test facility for the "Compact Linear Collider". Allowing for inevitable configurational uncertainties, good agreement is found between theory and experiment. In particular, the simulation predicts a substantial dependence of horizontal emittance ϵ_x on beam width (as controlled by the lattice β_x-function) at the compressor location, consistent with the experimental observations. Previous simulations (using TraFiC4*[**4**] and ELEGANT[**5**]) predict no such dependence. This dependence may be due to the centrifugal space charge force (CSCF)[**6**], a current-dependent and position-dependent coherent transverse force. The string space charge formulation avoids the renormalization step (subtracting the free-space space charge force) which is required (to remove divergence) in other methods. This means that coherent synchrotron radiation (CSR) and CSCF as well as all free space, space charge forces are included. This is in contrast with theories of emittance growth that, ascribing the growth entirely CSR, break down at low energy.

Emittance growth in a "standard chicane"[**13**] is also investigated. First to compare with other calculations—only modest emittance growth was observed, in agreement with previous determinations. Second, by comparing round and ribbon beams (like those actually needed in practice) to test whether the unexpected bunch shape dependence (described above) would give increased emittance for a 5 GeV beam as the beam height is reduced. (After correcting for halo generation, due to beam granularity in the simulation, and varying inversely with bunch height) the horizontal emittance, like both the momentum shift and the momentum spread, was found to be independent of bunch height. This is consistent with the emittance growth being dominated by CSR at high energy, as most workers have assumed.

1. Introduction

Many modern accelerator projects depend on preserving the (small) emittances of short intense electron beams produced by linear accelerators. These projects include FEL's (free electron lasers), ERL's (energy recovery linacs) and ILC (International Linear Collider) and CLIC (CERN Linear Collider). To produce short bunches these projects employ bunch compressing chicanes. Space charge effects in the magnets of these chicanes can degrade performance by causing emittance growth. Experiments at CERN using the CTF-II have provided substantial experimental data relevant to this issue.[**7**][**8**][**9**][**10**][**11**][**12**]

Emittance preservation is important for all of these projects. For FEL's, high phase space density is required to obtain stimulated emission, and short bunches are required for one class of x-ray experiments. For ERL's, ultrasmall transverse emittances are required to produce high x-ray brilliance. For CLIC, short bunches are required for good capture efficiency into the ultrahigh frequency drive linac. And for all linear colliders, such as the ILC, short bunches are required in order to be compatible with the tiny beam height at the collision point, which is needed for high luminosity. In all these cases there is a premium on preserving small transverse emittances.

Typical bunches from linacs can have (normalized) emittances of order 1 mm.mr, and the bunches are a few millimeters in length. These lengths can be shortened by two or more orders of magnitude by using magnetic chicanes. In a bunch-compressing chicane the beam suffers a +,–,+ sequence of bends, resulting in no net deflection. This causes a momentum-dependent shift $\Delta ct(\delta)$ in longitudinal coordinate ct of a particle (relative to bunch center); here δ is the fractional momentum offset. The parameter quantifying this effect is R_{56}, typically some tens of millimeters, with $\Delta(ct) = R_{56}\,\delta$ (to linear approximation.) The value of R_{56} is governed by the bend angles in the chicane. By running the electron beam "off-crest" through the linac, it is possible to produce a "chirped" beam for which δ is proportional to ct; $\delta = (d\delta/d(ct))\,ct$ (also to linear approximation). Working together, these two effects can convert a long bunch at the chicane input into a short bunch at the output.

The beam energies of the CTF-II electron beams are about 40 MeV. At this energy, though the electron speeds differ negligibly from c, the particles are not so stiff as to make free space, space charge forces negligible. The CTF-II references given above, especially [**12**], after discussing various influences on their observed data, conclude that CSR forces cause the qualitatively most striking aspects of their data. (It is because there is only CSR at wavelengths greater than the bunch length that CSR becomes important only for short bunches.) While agreeing with the importance of this force, the present paper also emphasizes the importance of conventional, non-relativistic, Coulomb forces, at the quite low energy of the data, and furthermore investigates the importance of the CSCF force, which can be regarded as the transverse counterpart of CSR.

Unlike the longitudinal self-force, the transverse self-force has a nonlinear dependence on transverse position in the bunch. This force is known to be an *even* function of the horizontal displacement[**22**][**23**], (at least for cases having the bunch long enough for the magnitude of the transverse fields to be proportional to the longitudinally-local charge distribution) The leading CSCF effect is therefore a steering (but no focusing) of the bunch as a whole. The leading nonlinear moment is sextupole. That such a force can cause horizontal emittance growth should not be surprising; it is the magnitude of the effect that needs to be determined. Furthermore, the field shape may be more complicated for short bunches.

The string space charge model is thoroughly described in references [**1**][**2**][**3**], and some recent refinements are described in the appendix to the present paper. The main idea is that the (appropriately-retarded) space charge forces simply cause intrabeam scattering. Each particle exerts an electromagnetic force on every other one. In this approach, with energy being conserved, the effects of radiation are implicitly incorporated by the "self-work" these charges perform on each other.

If it were computationally possible for a simulation to use 10^{10} particles no-one could take exception to this approach. But the highly singular $1/r^2$ Coulomb force is usually regarded as making this approach unworkable for simulations that (because of computation time) restrict the number of macroparticles to, say, 10^3. The occasional near encounters would give hopelessly erratic results if counter measures are not taken. To smooth this behavior a common approach is to take an intermediate step in which, using PIC (particle-in-cell) code, one evaluates effective fields (on a grid). In a subsequent step, deflections of individual particles are calculated by interpolation between points on the grid.

In the string approach, to suppress the close encounter divergence, each particles is treated as a longitudinally-aligned *string* (or needle) as regards the forces it causes. But the particle is treated as a *point* for purposes of determining its orbit. The dependence on (artificial) string length is suppressed by using small (but not too small) values. (The string can also be assigned a tiny height, making it a vertically aligned ribbon.) This computational approach scales poorly (as N_p^2, where N_p is the number of macroparticles) but, for a single pass through a relatively short beam line, a single laptop computer provides sufficient compute power for the calculations in this paper.

Because there is no need for renormalization (suppressing the divergence by subtracting the field-free force) the string calculation includes *all* free space, space charge effects. The formulation is also applicable to less-than-fully-relativistic charged particles. One qualification is necessary: the forces on particles just entering, or just leaving, a magnetic field region are not calculated correctly. Since this is just an "end effect", negligible for bunch lengths sufficiently short compared to the magnet length, this restriction is not expected to be important, especially for the not-very-relativistic energies relevant for the experimental comparisons in the first part of this report.

Because of the extreme complication of the SCR and CSCF forces, it would greatly aid the design of the various projects mentioned earlier, to distill out an empirical, phenomenological, parameterization of the dependence of emittance growth on the important parameters such as bunch charge, bunch dimensions, particle energy, lattice parameters and magnetic field. We have not, as yet, obtained any such parameterization. We specialize primarily to the CTF-II results.

An issue of special importance for this paper is dependence on transverse bunch dimensions. The relevant CTF-II measurements concern dependence on β_x (at the chicane location) with all other parameters held constant. According to reference [**12**] the TraFiC4*[**4**][1] and the ELEGANT[**5**] codes predict the emittance growth to be independent of β_x.[2] In reference [**12**], Braun et al. therefore register surprise, and state that they have no explanation for the strong dependence on β_x that they observe. Their data is shown below in FIG. 6, along with further discussion.

Using energy conservation, the energy emitted in CSR can be equated to the self-work done by the bunch force acting on itself. But this force is a function of longitudinal position in the bunch. Particles at the front of the bunch are actually accelerated and particles at the back of the bunch are decelerated enough to make up the total radiated energy. The conventional wisdom has been that transverse emittance growth is dominated by the betatron excitations induced with this longitudinal dependence. The strong dependence on β_x observed experimentally suggests that other factors are also important.

Another surprise noted by the authors of reference [**12**] is the absence of dependence on vacuum chamber height. This issue, important though it is, is *not* investigated in this paper.

---

[1]In this paper certain theoretical simulations of CTF-II results are described as using the code TraFiC4*. The intention of the asterisk is to provide the following warning. The TraFiC4* predictions come from the CTF-II papers, not directly from TraFiC4 authors. These simulations were performed a long time ago and, like all codes, TraFiC4 has evolved considerably in the meantime. In particular, a better modeling of the charge distributions has become possible due to the increased computer speed. The same comments apply to a lesser degree to simulations labeled ELEGANT. But then, as now, ELEGANT simply neglects all coherent transverse space charge forces.

[2]A basis for neglecting dependence on transverse beam dimensions is that, the characteristic ratio $\sigma_x^3/(R\sigma_l^2)$ being small compared to 1 (as it is), assures that the transverse bunch size is small compared to the distance over which the longitudinal CSR force is roughly constant.[**19**].

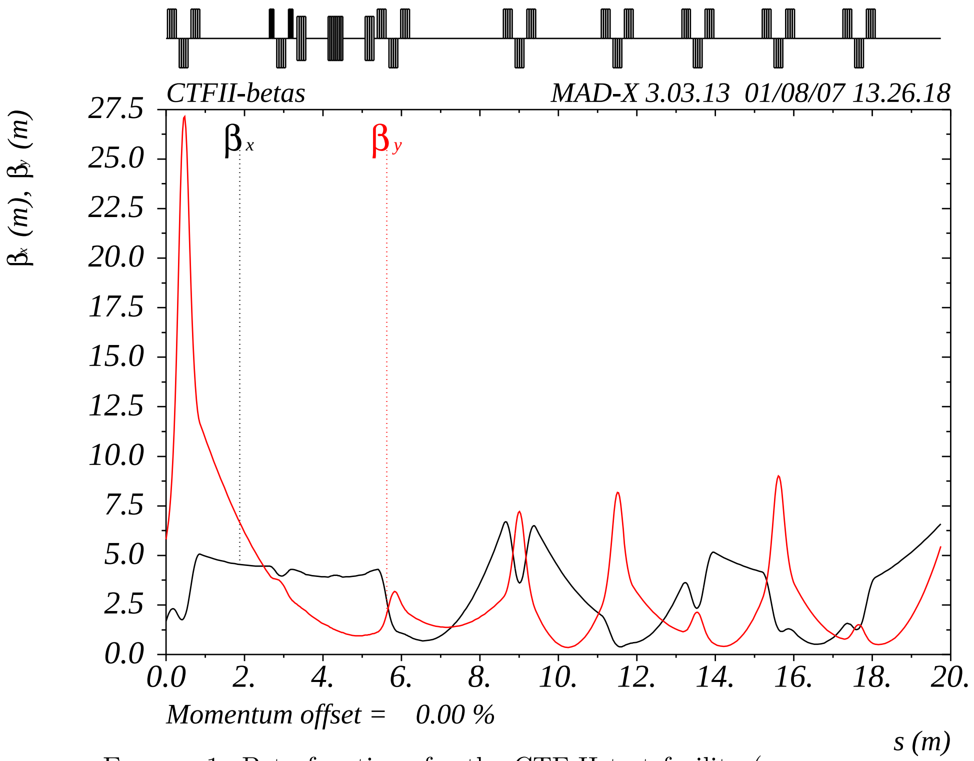

FIGURE 1. Beta functions for the CTF-II test facility (as reconstructed for $\beta_x = 4\,\mathrm{m}$ for this report).

2. Simulation Details

2.1. Lattice. A lattice description of (one variant of) most of the beamline used for the CTF-II experiments of 2001[**11**], was graciously provided to us by Lars Groening, in the form of a MAD lattice file. However a large matrix of lattices, for eighteen values of R_{56} and seven values of β_x (at chicane center) were required for this study. By design there were beam waists in both planes at the chicane center and β_y was held at 1.5 m for most data points. Ideally one would have used lattice description files from the original experiments. But these were possibly unavailable or, in any case, would have been hard to retrieve from the archives of the original experiment. Instead, lattices were tuned up at each point on the matrix of parameter values. As a result, even though the lattice functions at the chicane were accurately adjusted to the correct nominal values, the lattice functions (though sensibly regular and well-behaved) were undoubtedly different in the simulation than in the actual experiment. Because of emittance conservation in linear lattices, these deviations are not expected to be important.[3]

There are also other unknowns, such as off-crest linac phases, electron distributions, and mild deviations of the other lattice functions, α_x and α_y, from design, which introduce possible sources of deviation between theory and experiment.

Because of the large number of lattices requiring tuning, there was substantial possibility of error. In all cases, after tuning (typically six or nine of the quadrupoles

[3]There will be one comparison that is possibly sensitive to the lattice optics.

at once) using MAD8, the tuned-up file was automatically translated to MAD-X format using a python script. This step is necessary because UAL requires SXF format—a fully-instantiated lattice description format that can be output from MAD-X but not from MAD8. Finally the entire optics was re-checked in the UAL (finite element slice) environment. In every case the three MAD8/MAD-X/UAL lattice determinations agreed (to at least four decimal points) on all lattice functions and dispersions at the output (for identical inputs).

2.2. Relative Importance of Chromatic and Betatron Amplitudes. In order for a bunch compressor to function, there needs, initially, to be a correlation between momentum and longitudinal position. At this input point the dispersion $D(0)$ is zero *by design* in the experiment and *by definition* in the simulation. Subsequently the transverse particle amplitude can be decomposed into a betatron part, proportional to the square root of geometric emittance $\sqrt{\epsilon_{xn}/\gamma}$, and a chromatic part $D(s)\delta$, where $\delta = \delta p/p_0$. A chromatic factor $\mathcal{F}(s)$, defined by

$$\mathcal{F}(s) = D(s)\delta\sqrt{\frac{\gamma}{\beta_x(s)\epsilon_{xn}}}, \tag{1}$$

quantifies the relative importance of these two contributions.

It is especially important for $\mathcal{F}_{\rm MP}(s)$ to be small compared to 1 at the measurement point MP where ϵ_x is to be measured, since the entire horizontal amplitude there is ascribed to betatron motion in evaluating the emittance. For this report, since the square root factor is of order $\sqrt{10^5\,\mathrm{m}^{-2}}$, the factor $D_{\rm MP}\delta$ has to be held well below $10^{-3}\,$m. The non-vanishing of this factor is referred to as "dispersion leakage"; it can be quantified as a fraction of the maximum dispersion in the beam line. With the typical maximum dispersion being of order one meter, the dispersion leakage therefore has to be less than a part in a thousand.[4] [5]

It is also useful to evaluate $\mathcal{F}(s)$ at a point in the beamline (typically the center point of the chicane) where the dispersion is maximum. At this point the product $D_{\max}\delta_{\max}$ for a typical compressor at typical setting of R_{56} has a value of tens of millimeters, and the chromatic factor is roughly

$$\mathcal{F}_{\max} = \sqrt{\gamma}\sqrt{\frac{10^{-5}\,\mathrm{m}^2}{\beta_x(s)\epsilon_{xn}}}. \tag{2}$$

For values of β_x which leave this factor comparable to, or less than, 1, there is the possibility of space charge effects dependent on β_x.

There is credible evidence, especially near minimum bunch length settings, that radiative effects are most important near the end of the final chicane magnet. (This explains the negative peak in the curve of energy loss versus R_{56} at the value which minimizes the bunch length. Since the dispersion approaches zero asymptotically through the last magnet of the chicane, R_{56} is nearly zero for a substantial interval

[4]In a chicane for high energy (such as 5 GeV) electrons, the dispersion has to be canceled to higher accuracy than is true at 40 MeV. For the ILC, assuming a normalized emittance of 10 mm.mr, the fractional dispersion leakage has to be some thirty times smaller than in the CTF-II case.

[5]The procedure used in the present simulation to suppress spurious emittance growth would be invalid if $\mathcal{F}_{\rm MP}$ were comparable with or larger than 1. For chromatic part large compared to betatron part, the betatron part would contribute to the emittane only "quadratically", and subtracting the emittance calculated at reduced charge would leave a seriously underestimated betatron part.

there, which makes long the path length over which the bunch length is near its minimum value. This is what causes the observed negative peak.) In this region it is also true that the bunch transverse dimensions are dominated by its betatron amplitudes.

2.3. Simulation Procedures and Uncertainties. To the extent possible, electron beam parameters have been extracted from the references cited above, especially[**9**]. Part of the reason for concentrating on this series of experiments is their excellent planning, execution, and documentation. Nevertheless, some parameters have had to be based on empirically fitting theory to experiment. For example the input beam heights and angular divergences and the value of $d\delta/d(ct)$ are fixed fairly unambiguously in this way.

Since it is emittance growth that is of primary concern, the calculation of emittance is clearly of importance. Regrettably it is not so easy to be confident that emittances as defined in the simulation are consistent with their determination in the experiment. For vanishing momentum spread, if the lattice is "linear", both transverse emittances are conserved. This behavior was confirmed to high accuracy in the simulation. But, for the compressor to work, an energy offset correlated with longitudinal position is required.

The sorts of bunch distributions used are shown in Fig. 2. The number of particles per bunch was typically taken to be $N_p = 800$. Earlier runs with only 400 particles gave very similar results, as did a few runs with 1600 particles. In all cases the sides of the heavy rectangles mark projected r.m.s. values of the distributions. Input and output parameters are listed at the top of the figure, with output paramters in the fourth row. From the horizontal scale in this figure one sees that the bunch has, in fact, been shortened. As it happens Fig. 2, with $Q = 5\,\mathrm{nC}$, $R_{56} = 48\,\mathrm{mm}$, is something of a "worst case", as it shows a small, but unexpected, alteration of the vertical emittance.[6]

Because of contorted optics, the phase space shapes have been distorted away from ellipses. Such distortion can increase the emittance (as calculated), even in cases where the bunch charge is negligibly small, and even when only symplecticity-preserving forces are present. Any such growth of the emittance is an artifact of the method of calculating emittances. To some extent this effect can be monitored by inferring Twiss functions from the aspect ratio of the data and comparing their values with the values given by the lattice design. Unfortunately any such spurious growth depends on R_{56}, further complicating the interpretation of the data. There can even be some spurious emittance growth in the vertical plane from this source.

Another likely source of spurious emittance growth is the presence of dispersion at the lattice location where the emittances are measured. The analysis here assumes that the dispersion at that point is zero and ascribes the entire value of x for every particle to its betatron amplitude. For $R_{56} = 40\,\mathrm{mm}$ the dispersion at chicane center is about $0.13\,\mathrm{m}$ and, for the actual dispersion evolution program in use, the dispersion "leakage" at the emittance-determination point was about $10^{-4}\,\mathrm{m}$. For a momentum offset of 0.01, the linear dispersion contribution to x is of order $10^{-6}\,\mathrm{m}$ and the beam sigma is of order $\sigma_x \approx 1\,\mathrm{mm}$. Assuming the nonlinear chromatic effect is at most comparable, it seems safe to ignore this source of spurious horizontal emittance, both in the simulation and in the experiment.

[6]This is the result that may be influenced by uncertain lattice optics.

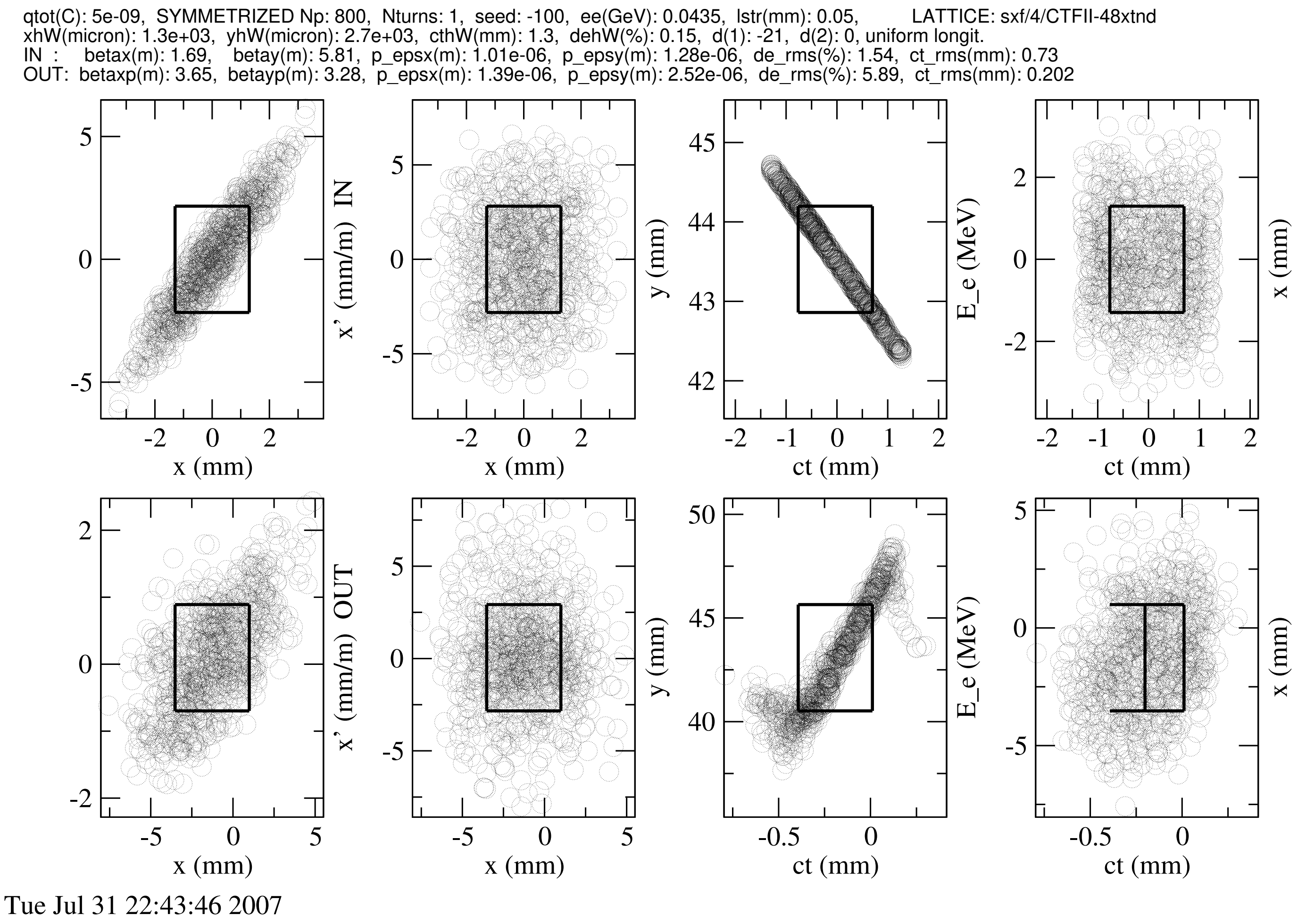

FIGURE 2. Particle distributions at the entrance and exit of CTF-II for $Q = 5\,\text{nC}$, $R_{56} = 48\,\text{mm}$. This is one of the extreme examples of (unexpected) growth of vertical emittance.

When a beam emittance is calculated as the r.m.s. value of the Courant-Snyder invariants of the individual particles the result depends on the values (presumably obtained from a linear lattice model) of the Twiss functions of the lattice at that point. From a perturbative point of view this is a sensible approximation. But the emittance, technically speaking, should not depend on the lattice functions. An alternative formula for the emittance is

$$\epsilon_x^2 = < x^2 >< x'^2 > - < xx' >^2 \,. \tag{3}$$

In our simulations both of these procedures exhibit spurious emittance growth (i.e. for $Q \approx 0$), but we find that the latter (in principle better justified) produces less spurious emittance growth. We therefore use Eq. (3) in our subsequent analyses.

What is to be done about spurious emittance growth for the present analysis will be discussed shortly, in connection with discussion of theory/experiment comparisons. Let it be noted here, though, that charge-independent phase space distortion provides a worrisome potential source of spurious emittance growth, both in simulations and in experimental emittance measurements.

Being based on a Monte Carlo simulation, the results in this report depend on an initial seed. Some results (such as ratios of outputs for two different R_{56} values) are quite insensitive to the choice of seed. But others (especially absolute emittance growth) are quite sensitive. Apart from limiting the accuracy of the predictions, this complicates the interpretation of internal consistency checks (such as studying dependencies on number of macroparticles N_p or string length $l_{\mathrm{str.}}$). Because of the strong dependence on bunch length, the lumpiness in longitudinal charge distribution due to the relatively small number of macroparticles may be an important source of fluctuation. Initializing longitudinal particle coordinates on a regular grid, rather than randomly, has been found to reduce this source of fluctuation noticeably in some cases.

In the true physical situation a particle is subjected to an almost continuously varying space charge force. But, within the simulation, this smooth force is modeled by a vast number of tiny momentum impulses. This is a rich source of randomness and provides, as it turns out, the dominant source of halo generation. This issue will be discussed further in connection with the standard chicane.

2.4. Experimental Procedures and Uncertainties. The various publications from the CTF-II project describe many experimental consistency checks performed in the progress of their investigations. An especially-to-be-feared source of error would be the existence of nonvanishing dispersion at the emittance-measuring location. The chicane, made from three (or four if the center bend is split) "rbend" magnets, in principle introduces no dispersion. This they confirmed experimentally. They do however acknowledge the presence of a longitudinally-asymmetric bunch distribution and the possibility of fluctuation in the input parameters, especially to account for the less good correspondance between experiment and theory for their $Q = 10\,\mathrm{nC}$ data than for their $5\,\mathrm{nC}$ data.

Though the issue seems not to be emphasized in their publications, the same difficulties as the simulation has in determining transverse emittances seem likely to complicate the experimental determination. The extent to which this was investigated experimentally is unclear. It could have been done, for example, by measuring (spurious) emittance growth, for bunch charge as small as practicable, as a function of R_{56}.

3. Dependence on R_{56}

In this section comparisons, as functions of R_{56}, are made between simulations and data. The parameter choices correspond to the CTF-II data described in reference [**9**]. All data in that report are reproduced here, with the exception that output momentum distributions are represented only by their r.m.s. widths rather than being displayed in detail. Complete sets of simulated data were taken at each of two values of charge per bunch Q, namely 5 nC and 10 nC. For 5 nC, dependence of output momentum p_0, and its r.m.s. spread Δp, as well as the bunch length σ_l, are shown in FIG 3. All three data sets, CTF-II, TraFiC4*, and UAL are in quite good agreement. Whatever disagreement there is can probably be blamed on deviant calibrations, especially of the R_{56} scales, and the location of, and minimum bunch length value achieved (both of which depend on assumptions concerning the distributions of the initial electron beam, and on a possibility noted in the caption to the figure). Values of the transverse emittances, renormalized as described next, are also shown. In this case the horizontal dependence is essentially unaltered by the renormalization. The vertical emittance growth is substantially reduced, but not removed, by the renormalization.

The discussion here proceeds from the concept of *spurious* emittance growth introduced in Section 2.3. For each scan, a similar scan is taken for a vanishingly small value of Q (where "vanishingly small" in this report may mean $Q = 0$ or "value of Q is reduced by a factor of 1000".) These negligible-charge scans can exhibit appreciable "emittance growth" which is obviously spurious. The source of this growth was described previously. The *renormalized* simulation points were taken by simply *dividing* the Q-data by the reduced-charge data. By taking this ratio there is no spurious emittance growth *by definition.* But a penalty attending this approach is that the absolute normalization is lost and has to be restored empirically. Since the absolute normalizations are quite good for small values of R_{56}, this renormalization does not distort the data very badly. Spurious horizontal emittance growth seems to be reduced somewhat by the symmetrization procedure described in the appendix.

An alternate analysis is to *subtract* the reduced-current emittances from the full-current emittances and plot $\Delta\epsilon_x$ and $\Delta\epsilon_y$. This amounts to much the same thing as the procedure described above, except normalized to the ideal (pre-compressor) distribution rather than to the (post-compressor) distorted distribution. Comparisons produced this way are quite similar to those shown.

After this processing, the UAL simulation predicts little emittance growth in either transverse plane. In this 5 nC case, the UAL and TraFiC simulations are in quite good agreement with the data. Possibly contrary to expectation (based on the assumed CSR-dominance) the vertical emittance is more affected than the horizontal. Attempts to account for this will be discussed later.

FIG. 4 shows the same distributions for $Q = 10$ nC. Again, after renormalization, the UAL simulation exhibits relatively little emittance growth in either plane. In this regard there is serious disagreement with the TraFiC4* simulation, which shows substantial horizontal emittance growth. On the other hand, TraFiC4* mimics well the observed negative peak in output momentum at $R_{56} \approx 30$ mm in the 10 nC data. It can be noted though that, if one accepts the experimental error bars literally, the UAL simulation disagrees with the data only modestly—all data points are within two sigmas of the simulation's prediction. There is relatively good

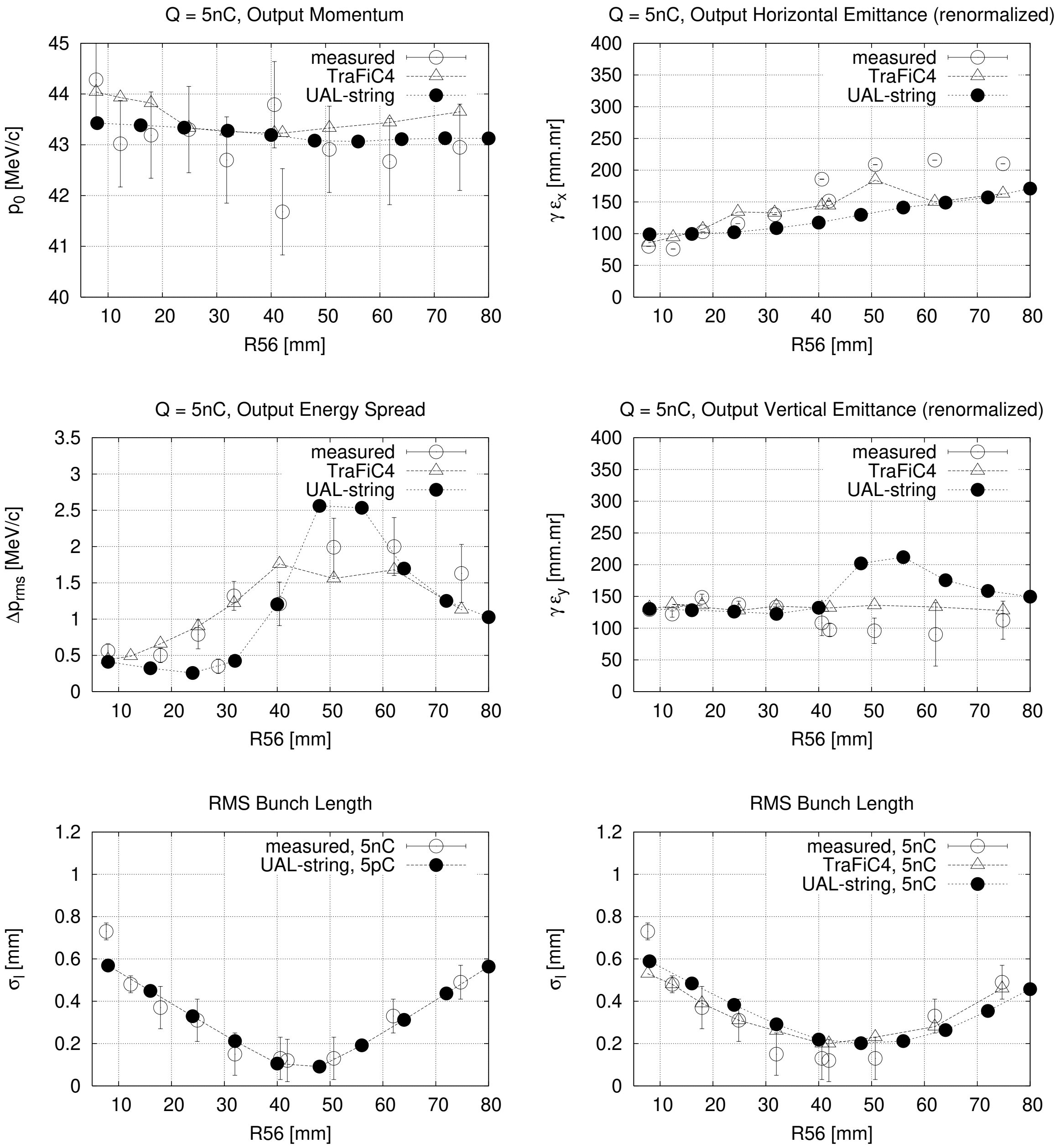

FIGURE 3. $Q = 5\,\mathrm{nC}$ output momentum, energy spread bunch length and emittances. The conversion from "raw" to "renormalized" is discussed in the text. In the bottom graphs the simulations predict a bunch length dependence on bunch charge Q near the minimum. The deviations visible in these graphs suggest that the system parameters (fit empirically without accounting for this dependence) may not be quite right. Is it possible the experimenters *tuned* to minimize the bunch length at the minimum at $Q = 5\,\mathrm{nC}$ rather than at $Q = 0$?

CTF-II/TraFiC/UAL agreement on the peaked-dependence of Δp_{rms} and on the (absence of) vertical emittance growth. Further interpretation and comment on these plots is deferred to Section 7.

4. Dependence on Longitudinal Position

Dependence, on longitudinal position, of momentum spread Δp and bunch length σ_l, is shown in FIG. 5. In this case there are no experimental data points (because there are no sensors along the beam line), but this data can be compared with FIG. 7 in reference [**9**] (not reproduced here), which shows results from the TraFiC4* simulations. The slightly discontinuous horizontal scale of FIG. 5, and non-matching parameter values, complicates this comparison. But the agreement between UAL and TraFiC4* is excellent. Basically the bunch shortens in the chicane and preserves its bunch length from then on. On the other hand the energy widths grow continuously after the chicane. The growth is proportional to path length and depends on the bunch length. For the value of R_{56} that minimizes σ_l the growth rate of Δp is maximal.

The growth of Δp with s can be explained analytically, with no need for simulation. Particles near the front of the bunch are pushed forward by the intrabunch Coulomb force within the bunch and particles near the back are pushed back. Since all particles are traveling at the same speed these forces have no effect on the bunch length but they do affect the spread of energies. For values of R_{56} below that at which the bunch length is minimized the particles near the front of the bunch have the reduced energy they (intentionally) had coming out of the linac. In this region the energy spread therefore *decreases* with increasing s. For values of R_{56} above that at which the bunch length is minimized the longitudinal phase space has been *over-rotated*, so the particles at the front have excess energy. In this region the Coulomb force increases the energy spread, though more weakly in cases where the bunch length is long.

5. Dependence on β_x at Chicane Center

To investigate how emittance growth depends on transverse bunch size, the CTF-II group took data over a series of lattices that differed only in the value of β_x at the center of the chicane.[**11**][**12**] This data, along with the UAL and TraFiC4* and, in one case, the ELEGANT simulations, are shown in FIG. 6. To generate these graphs simulations were run, for each of several values of β_x, for fixed values of R_{56} ranging from minimum (little bending in the chicane magnets) to maximum (large bending in the chicane magnets).

It is curious that a fractionally stronger effect is measured for 4 nC (bottom graph) than for 9 nC. This may be due to the minimum bunch length being less (though nominally they are equal) or the absolute emittance at 4 nC being less, which it is. In any case, the absolute increase in emittance growth over the full range of β_x values is comparable in all cases. These data disagree qualitatively with the absence of dependence predicted by TraFiC4* and ELEGANT. But it is in semi-quantitative agreement with the UAL string calculation.

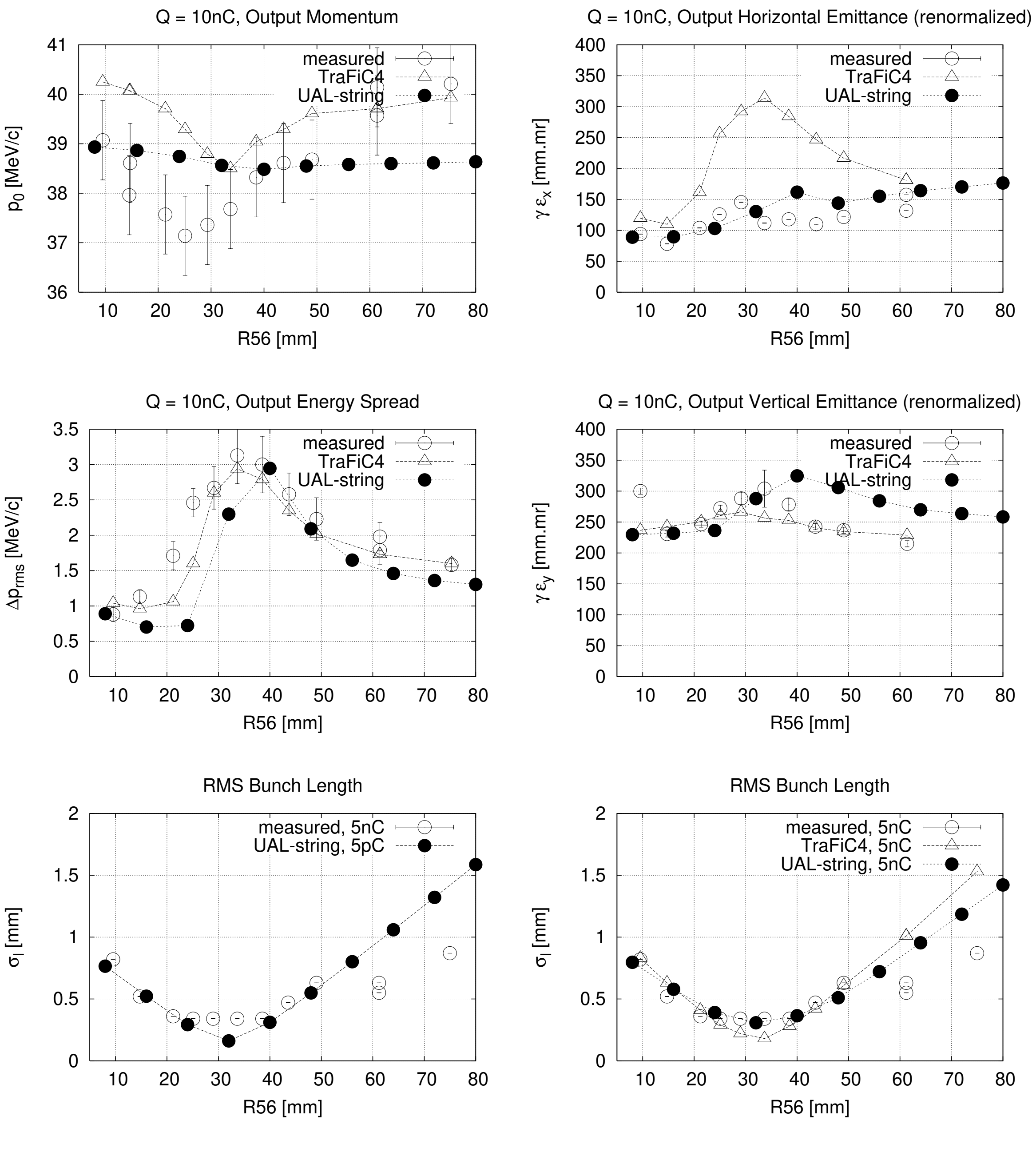

FIGURE 4. $Q = 10\,\text{nC}$ output distributions. Deviations near the minimum were discussed along with the $5\,\text{nC}$ data. These simulations used 800 particles, but results with 400 particles seemed essentially equivalent.

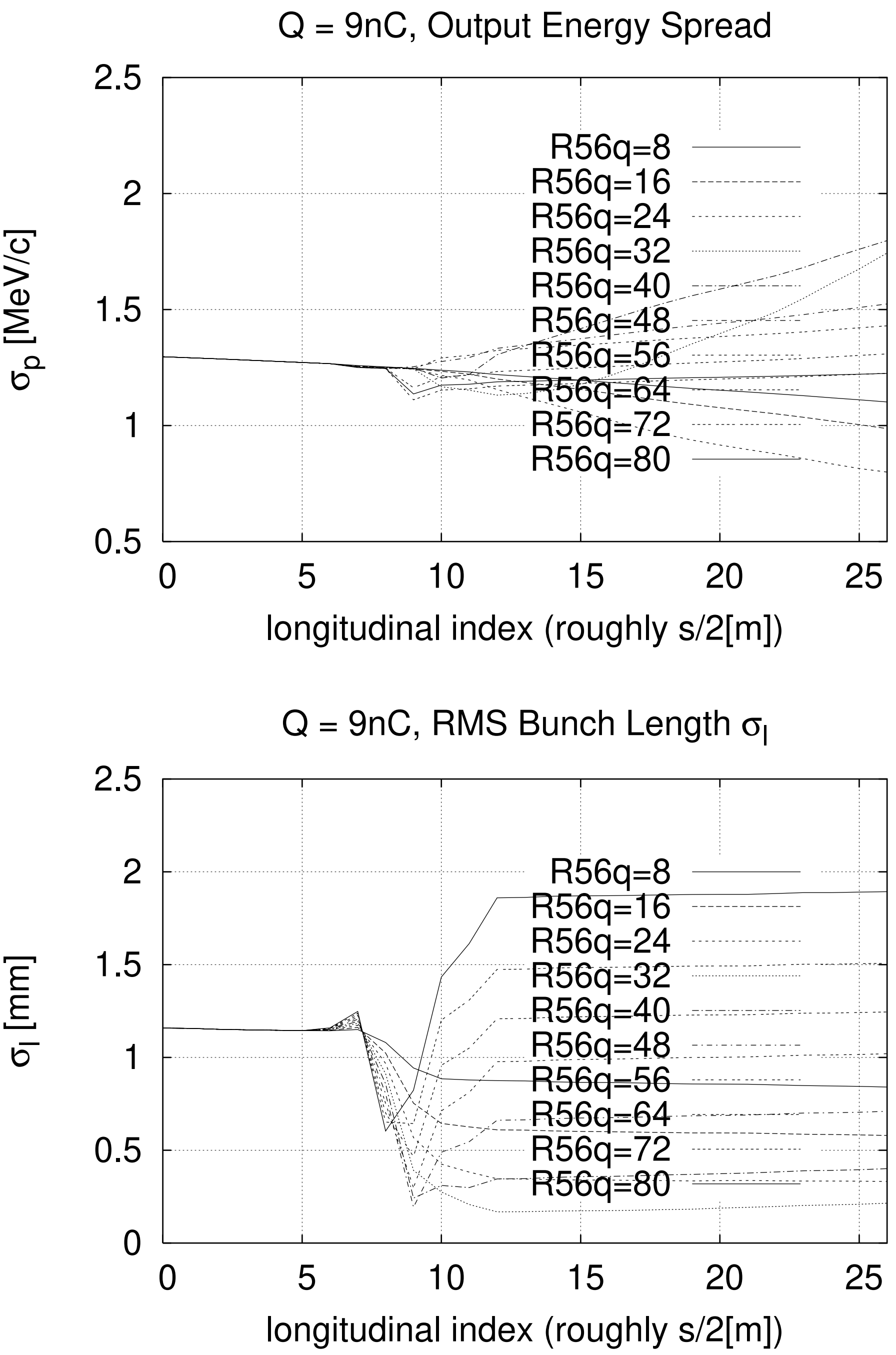

FIGURE 5. Dependence on longitudinal position of momentum spread Δp and bunch length σ_l. The chicane magnets are at index location 6, 8, 9, and 11 and other index locations are spaced more or less uniformly at 0.5 m intervals.

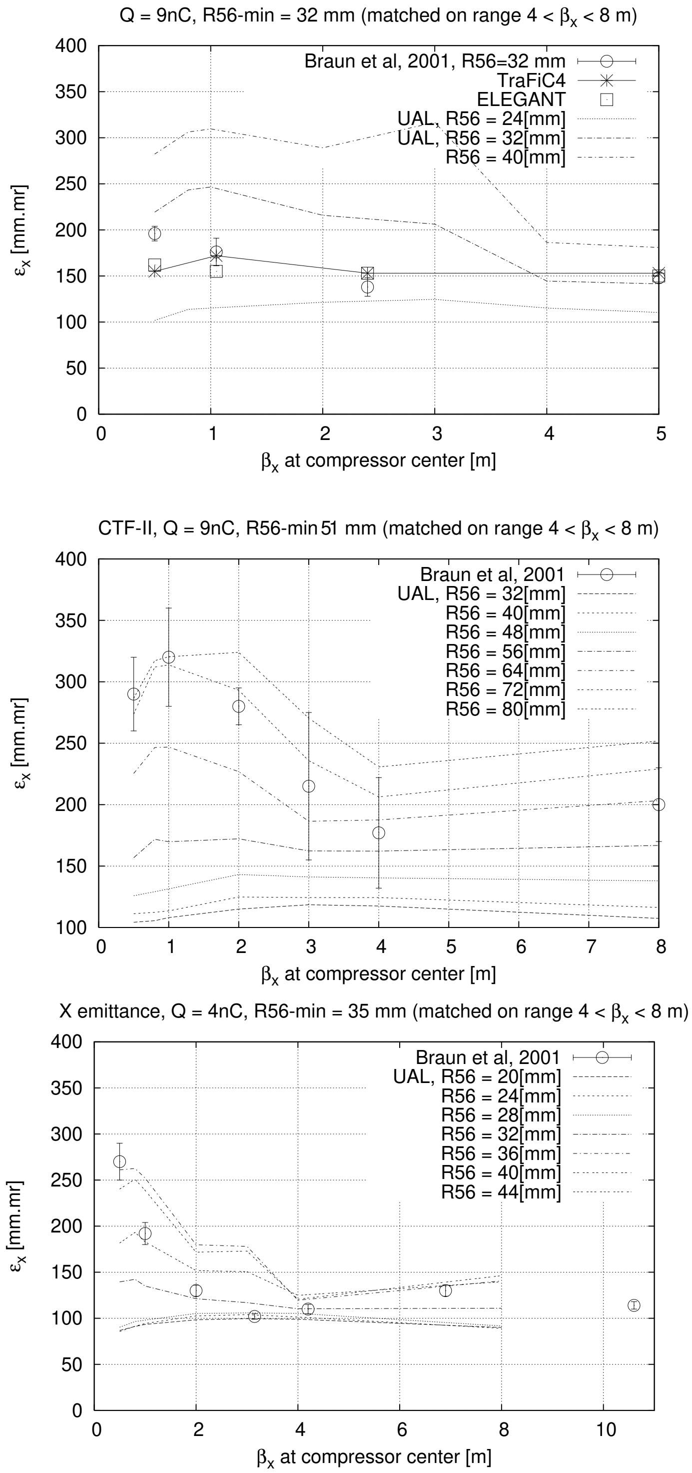

Figure 6. Measured and calculated dependence of horizontal emittance on β_x at chicane center for three different parameter combinations. Open circles are measured values, smooth curves are UAL string calculations. TraFiC4* and ELEGANT (upper graph only) simulations predict "no significant dependence on the beta function"[**12**].

6. Emittance Growth in the "Standard Chicane"

A so-called "standard chicane", for 5 GeV electron beams, was introduced in a 2002 workshop on coherent synchrotron radiation[**13**]. This was intended to enable benchmark comparisons of the various methods and computer codes. Bunch compressor emittance growth results are reviewed by Giannessi.[**17**] A selection of his results most relevant to the current paper are tabulated in Table 1, which is copied from the original, but with a row added at the bottom and a column on the right, giving the results of the "UAL stringsc" code. In all cases (except for the final column) standard parameter values are used, as given, for example, by Emma[**14**]. The table shows quite good agreement among the various determinations for the nominal "round beam" parameters.

It is the entry in the final column that will be considered especially here; this entry comes from reducing the vertical emittance by two orders of magnitude from its nominal value. (Properties of ribbon beams are of more than academic interest, since most applications of low emittance beams require $\epsilon_y \approx \epsilon_x/100$.) In this revised configuration the intepretation of the simulation resulats cannot be separated from the discussion of "halo generation" and on the dependence on the string length and string height of the string space charge model.

The standard chicane parameter values can be read from the data at the top of the graphs shown in Fig. 6 which shows phase space distributions of the particles at input to and output from the compressor. The distributions in this figure are not entirely typical in that, to produce a more easily interpretable benchmark, the uncorrelated input energy spread has been set to a very small value. Potential sources of "disagreement" between standard chicane and CTF-II behavior can be inferred by close comparison of this figure with Fig. 2—here the longitudinal distribution is Gausssian and gridded, not uniform and random. Like the earlier figure, this figure is also a "worst case". Here because the beam height has been reduced by a factor of ten to produce a ribbon beam, in order to pictorially exhibit the halo production predicted by the simulation.

Numerous comments about these data can be based on the graphs in Fig. 8. The bottom right figure shows the bunch length as a function of R_{56}; only one case is shown as, at such high energy, there is little dependence of bunch length on bunch charge or transverse dimensions. Especially noteworthy, however, is the fact that a relatively small upward shift (from $R_{56} = 25\,\mathrm{mm}$ to $R_{56} = 28$) produces close to an order of magnitude reduction in bunch length.[7] This is not so surprising; presumably the nominal chicane parameters have been adjusted to be just below the point where bunch head and tail can change places. But nearness to this "Jacobian singularity", at the point where the bunch length is minimum, undoubtedly contributes to the scatter of calculations like those in Table 1. (In actual practice the uncorrelated energy spread would probably be much greater than is assumed in the nominal benchmark parameter set and the bunch length minimum would be far less sharp.) The figures in the middle (up-down) of the page, shows that the mean energy shift is substantially increased at the bunch length minimum (though the fractional shift is not large even at that point.) This shift is independent of the vertical emittance. This is as expected—the shift is due to CSR, which is essentially independent of transverse bunch dimensions.

---

[7]Incidentally, the fact that the bunch length for the $R_{56} = 28\,\mathrm{mm}$ case is not large compared to the string length, makes the computed results unreliable in that case.

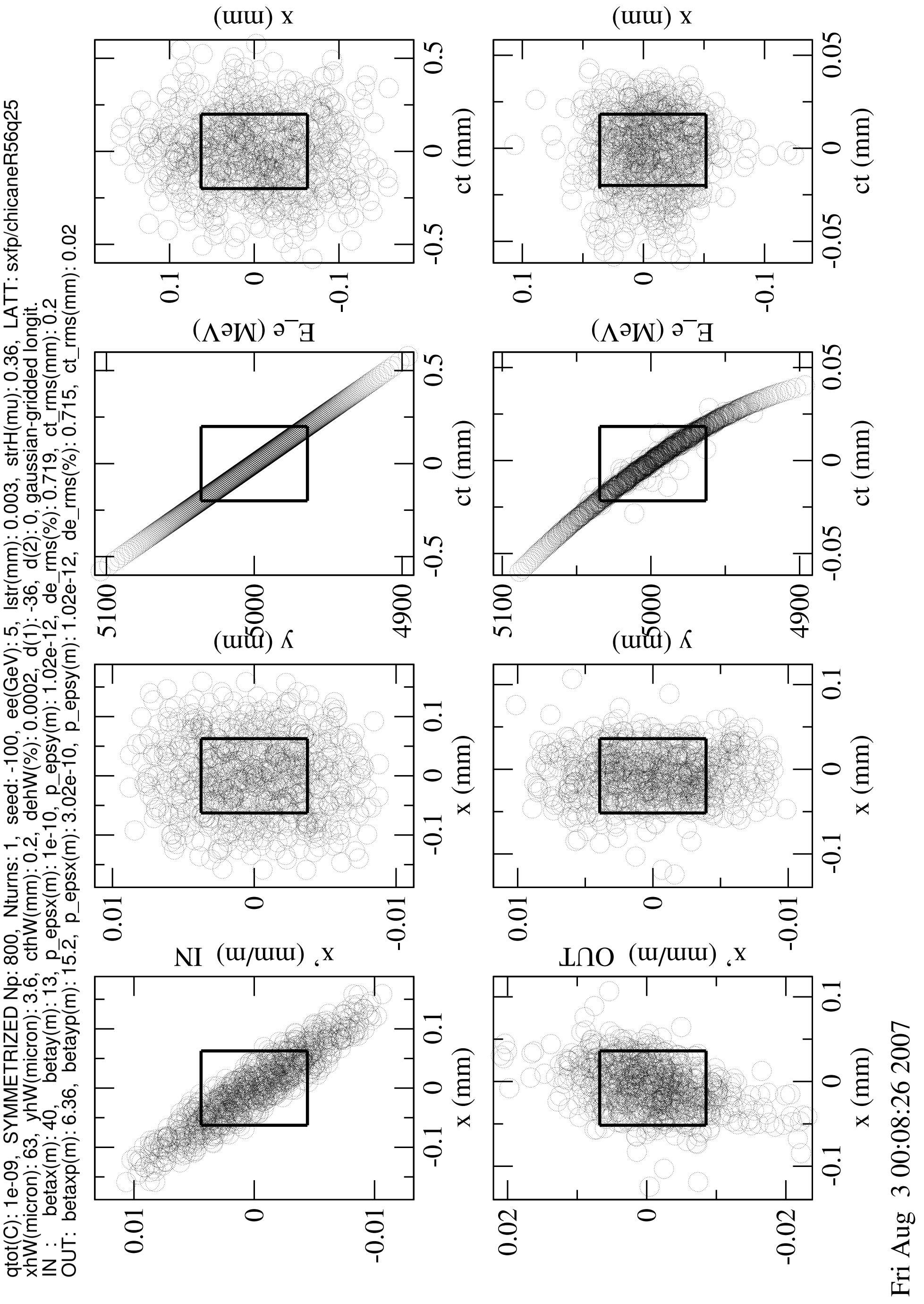

FIGURE 7. Particle distributions at the entrance and exit from the "standard chicane" benchmark;[**14**] However, to make the "halo" visible (in the bottom row, third plot over) the vertical emittance $\gamma\epsilon_y$ has been reduced to 0.01 mm.mr from its nominal value of 1 mm.mr.

Table 1. List of benchmarked codes giving the beam parameters at the output of the chicane (from Giannessi).[**17**] Results in the bottom row are from the present simulation. The first term in the sums indicated by asterisks is ascribable to the "beam core". The second term is ascribable to the "beam halo" in the simulation, which is probably a numerical artifact coming from granularity in the beam. This emittance increase would, in any case, have little effect on luminosity in colliders or beam brilliance in x-ray sources. It is unclear whether a distinction between core and halo would be appropriate for any of the other entries in the table.

Dimension	Code Name	ΔE %	$\Delta\sigma_E$ %	$\gamma\Delta\epsilon_x$ mm.mr	$\gamma\Delta\epsilon_x$ $\epsilon_y = 0.01$mm.mr
3D	TRAFIC4	-0.058	-0.002	0.4	
3D	TREDI	-0.041	0.017	1.3	
3D	Program by Li	-0.056	-0.006	0.32	
1D Line charge	ELEGANT	-0.045	-0.0043	0.55	
1D Line charge	CSR_CALC	-0.043	-0.004	0.52	
1D Line charge	Program by Dohlus	-0.045	-0.011	0.62	
3D	UAL stringsc	-0.028	-0.0049	$(0.18+0.17)^*$	$(0.26+3)^*$?

It will be seen shortly that "halo particles" are contributing substantially to the data plotted in the upper right figure in Fig. 8, giving the horizontal emittance growth as a function of R_{56} for the ribbon beam, but they have little effect on the other plots.

6.1. Dependence on String Parameters and on Beam Aspect Ratio. In principle the result of the simulation should be independent of number of macroparticles *np*, number of intervals *nsplit* into which the bends are segmented, and of the string dimensions $l_{\rm str}$ and $strH$, with the latter two values having been varied systematically until independence is achieved. Fig. 9 shows dependence on *np*; all curves have flattenned out for values of *np* exceeding 400 or so. Fig. 10 shows dependence on $l_{\rm str}$. In all cases here, the product *np.nsplit* was large enough to strongly suppress the generation of halo particles. (The significance of the product *np.nsplit* is that the maximum close-encounter impulse is proportional to the macroparticle charge and to the longitudinal interval being represented in the numerical calculation—this is more fully explained below.) All *longitudinal* parameter determinations are essentially independent of $l_{\rm str}$. See Table 2, which collects data from a few computer runs and gives their statistical fluctuations. For entries in this table $Q = 1\,$nC, $R_{56} = 25\,$mm, with nominal, round beam height 36 microns and "ribbon beam" vertical height 3.6 microns. Numbers in parenthesis in the first column give the number of independent runs that have been combined.

Most of what follows concerns the upper two graphs of Fig. 10 which show ϵ_x for the round beam (on the left) and ribbon beam (on the right). For now the only feature to be noticed is that, for short string length $l_{\rm str} = 2\,$microns, the horizontal emittance increase is much greater for the ribbon beam than for the round beam. This behavior is exhibited in greater detail in Fig. 11 which shows, in the ribbon beam case, the dependence of ϵ_x on the factor $1/(np.nsplit)$ for a few values of $l_{\rm str}$. The $1/(np.nsplit) \to 0$ limit of the horizontal scale is equivalent to the macrobunch

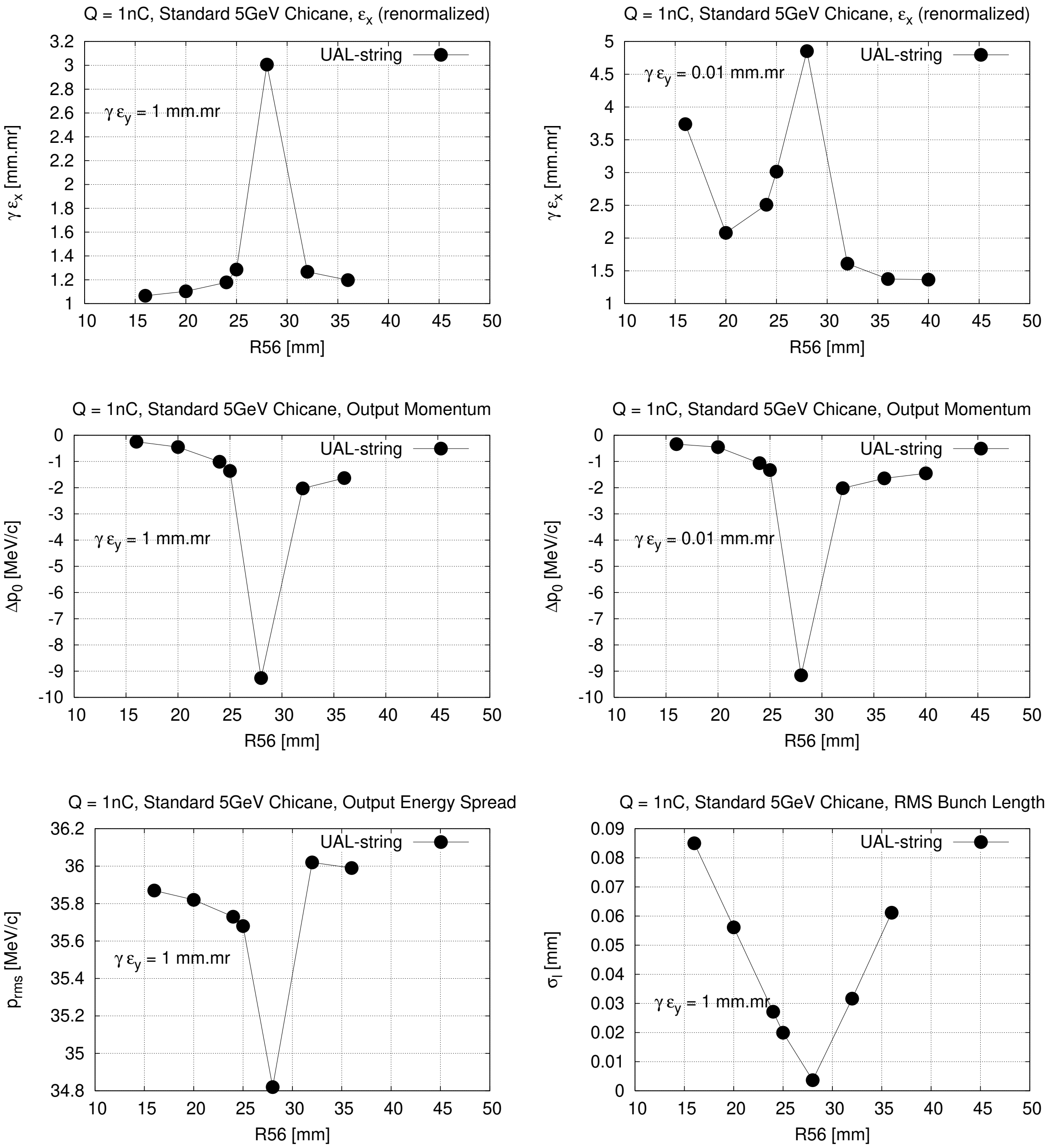

FIGURE 8. Dependence on R_{56} of various beam properties for round and ribbon beams. In all cases the electron bunch shape was Gaussian-gridded, the string length was $l_{\rm str.} = 3\,$micron, $\gamma\epsilon_{x0} = 1\,$mm.mr, $np = 800$, and $nsplit = 4$. Round beam, $\gamma\epsilon_y = 1\,$mm.mr, cases are shown on the left. The top two graphs on the right apply to the ribbon beam, $\gamma\epsilon_y = 0.01\,$mm.mr. As explained in the text, much of the horizontal emittance growth in the ribbon beam case is due to halo particles. The lower right figure shows bunch length for the round beam; the ribbon beam curve is essentially identical.

yhW micron	$l_{\rm str}$ micron	n_p	$n_{\rm split}$	$1/(n_p n_{\rm split})$ $\times 10^{-3}$	δE MeV	$\delta\sigma_E$ MeV	$\gamma\epsilon_x$ (raw) mm.mr	$\gamma\epsilon_{x0}$ mm.mr	$\gamma(\epsilon_x - \epsilon_{x0})$ mm.mr
36	3(4)	800	8	0.156	-1.386±0.009	-0.2476±0.0037	1.165	0.981	0.183±0.019
	3(4)	800	4	0.313	-1.377±0.002	-0.2529±0.0020	1.145	0.967	0.177±0.059
	3(4)	800	2	0.625	-1.368±0.018	-0.2488±0.0090	1.333	0.982	0.351±0.155
3.6	3(4)	800	16	0.0781	-1.40±0.018	-0.243±0.002	1.330	0.982	0.348±0.087
	3(4)	800	8	0.156	-1.39±0.008	-0.234±0.010	1.372	0.996	0.441±0.101
	3(2)	1600	4	0.156	-1.43±0.014	-0.244±0.015	1.568	0.999	0.507±0.088
	3(4)	800	4	0.313	-1.40±0.016	-0.226±0.013	1.671	0.996	0.692±0.114
	3(4)	800	2	0.625	-1.39±0.059	-0.223±0.030	3.184	0.982	2.201±1.180
3.6	4(2)	800	16	0.0781	-1.38±0.01	-0.239±0.012	1.184	0.996	0.198±0.013

TABLE 2. Output bunch parameters for the standard chicane with nominal parameters. All beam measures except ϵ_x are essentially independent of all variables exhibited.

charge being zero, which eliminates the production of halo particles by single close-encounter scatters. Naturally, the numerical accuracy suffers in this extrapolation, but the extrapolated values are consistent with being independent of $l_{\rm str}$..

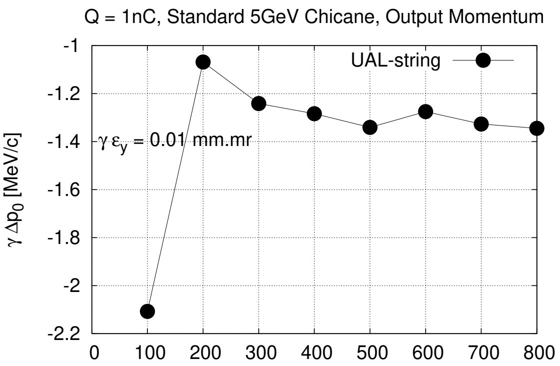

(a)

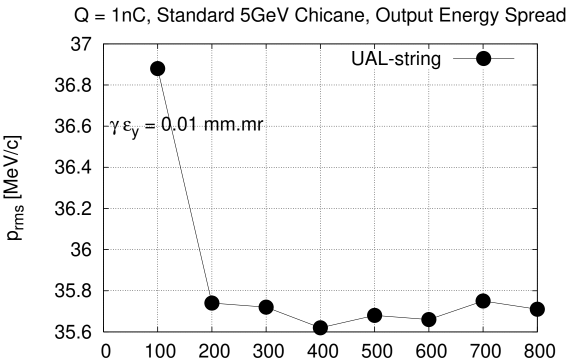

(b)

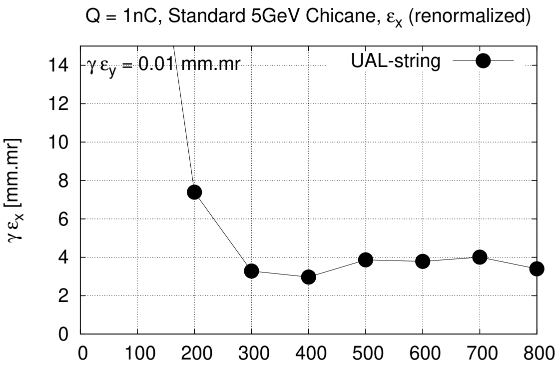

(c)

FIGURE 9. Dependence on the number of macroparticles, np, of various simulation outputs. In all cases $Q = 1\,\text{nC}$, $R_{56} = 25\,\text{mm}$, $\epsilon_{x0} = 1.0\,\text{mm.mr}$, $\epsilon_{y0} = 0.01\,\text{mm.mr}$ (ribbon beam). Round beam ($\epsilon_{y0} = 1\,\text{mm.mr}$) plots are similar.

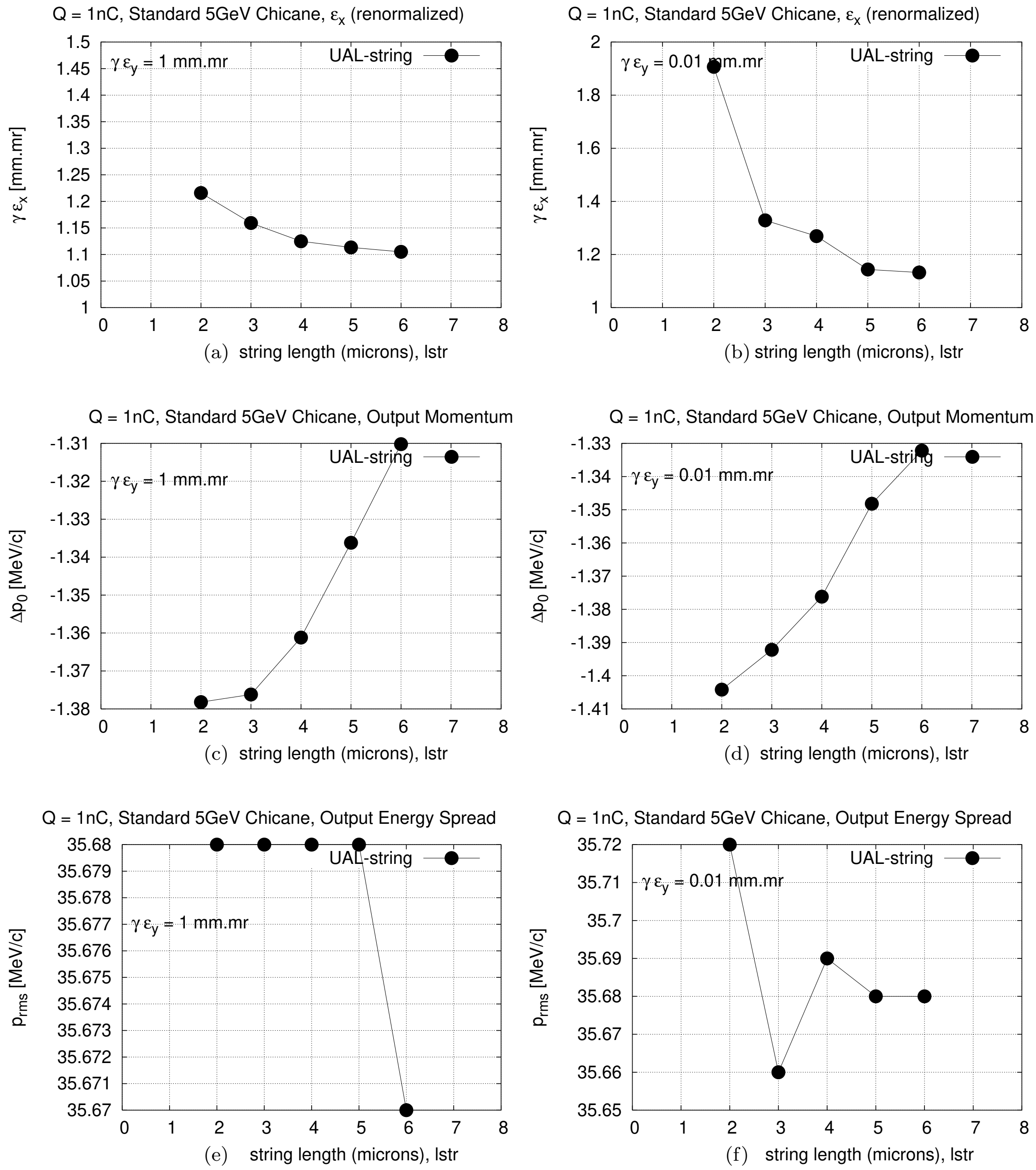

FIGURE 10. Dependence on the string length $l_{\rm str}$ for round and ribbon beams. In all cases $Q = 1\,$nC, $R_{56} = 25\,$mm (giving $\sigma_{ct} =$ 20 microns), and $\gamma\epsilon_{x0} = 1.0\,$mm.mr, $np = 800$, and $nsplit = 16$, giving $1/(np.nsplit) = 0.078 \times 10^{-3}$ For the figures on the left, $\gamma\epsilon_{y0} = 1\,$mm.mr; for the figures on the right, $\gamma\epsilon_{y0} = 0.01\,$mm.mr.

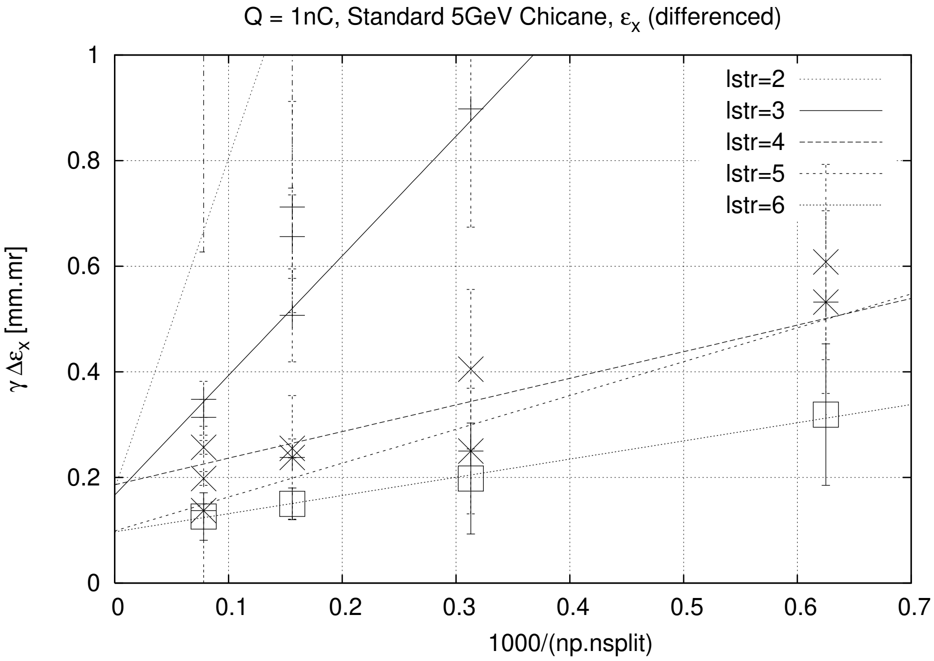

FIGURE 11. Dependence on $1/np/nsplit$ of the measured horizontal emittance growth $\gamma\Delta\epsilon_x$, for various values of string length $l_{\rm str}$, for a "ribbon" beam, with $\gamma\epsilon_y = 0.01$ mm.mr. For these simulations the string height $h_{\rm str} = yhW/10 = 0.36$ micron. Extrapolatation to the origin (infinitesimal charge per bunch) eliminates close-encounter halo production. Some residual dependence on $l_{\rm str}$ cannot be excluded but, in any case, it can be seen (comparing with Table 1) that reducing the beam height has not led to increased horizontal emittance growth.

7. Interpretation of the Results

7.1. Comparisons with CTF-II Data. (1) There is qualitative disagreement between CTF-II data and the UAL string simulation about the negative peak in p_0 in the 10 nC data of Fig. 4. As regards this feature, there is *qualitative* agreement between TraFiC4* and the experimental data. But, as noted previously, only a generous interpretation of the experimental error bars is needed for all theory and experiment points to be regarded as compatible.

(2) The CTF-II beam line differs from the standard chicane in that it has a long bend-free region following the chicane. (See Fig. 1 and Fig. 5.) This is relevant to the following comment. Experiment and simulation (both UAL and TraFiC4* and, presumably, ELEGANT) agree on the inexorable growth of momentum spread Δp in the drift region following the chicane, with the growth rate being dependent on bunch length (and even negative for small R_{56} values). As discussed earlier this behavior can be understood as reflecting longitudinal electrostatic Coulomb repulsion, not CSR. The standard chicane simulations show no such energy spread increase—rather they indicate a reduction in energy spread. This difference can be ascribed to the long bend-free region following the chicane in the CTF-II case; there is no such bend-free region in the standard chicane case.

(3) The shrinkage of vertical emittance observed in the CTF-II experiment may be spurious. No such change of vertical emittance is seem in the TraFic4* simulation. Both CSR and CSCF give only horizontal forces which cannot produce such vertical emittance changes. If the vertical emittance changes are *not* spurious they must be due to the same ordinary, Coulomb space charge forces that dominate low energy bunch size behavior. The focusing effect of Coulomb forces are known to produce phase space alterations that can cause the effective beam emittance to change, either up or down.

As it happens the UAL simulation shows an alteration of vertical emittance of the observed shape (i.e. setting in at values of R_{56} greater than the value for which the bunch suffers the turmoil of head and tail switching places); but the prediction is *growth* rather than the observed *shrinkage*. The leading effect of space charge at low energy is focusing. Since the effect of this focusing depends on the optics, this can cause either growth or shrinkage of the measured emittance. As mentioned earlier, the gross optics of our simulation may differ from the actual experimental optics, which, at least of the level of wishful thinking, could undo this discrepancy.

Otherwise all of the measured CTF-II values are reasonably consistent with the UAL simulation. The same cannot be said for the TraFiC4* simulations, which appears to overestimate the horizontal emittance growth of the 10 nC data.

(4) The most striking disagreement among CTF-II simulations concerns the dependence on bunch width, shown in Fig. 6. ELEGANT and TraFiC4* predict independence from β_x. The UAL simulation predicts increased horizontal emittance at small beam width, perhaps due to CSCF. In any case the simulation is in qualitative, one might even say semi-quantitative, agreement with the measured data.

The authors of reference[**12**] state: "Finally, the emittance growth due to uncompensated Talman-forces [another name for CSCF] for short bunches[**20**] was estimated. It increases with the beam size as well, and cannot explain the observations." The present simulation is not consistent with this statement.

7.2. Interpretation of Benchmark Chicane Results. Using Poynting vector methods, Schwinger[**21**] has calculated the properties of both incoherent and coherent synchrotron radiation. Most of the properties of the radiation *per se* have been amply comfirmed by subsequent experiments. In Schwinger's calculation the electron bunches are taken to be needle-shaped, with charge distributed uniformly along their length, and with vanishing transverse dimensions. Since CSR is strongly dependent on the longitudinal bunch distribution, Schwinger's formulas cannot be applied directly to the Gaussian longitudinal bunch shape specified for the standard chicane.

The total energy radiated from an electron bunch, both coherent and incoherent, is uncontroversial, and the dependence of the longitudinal self-force (wake field) on longitudinal position is also quite well understood. For example, the longitudinal force is essentially independent of transverse position in the bunch for the needle-shaped bunches of current interest. This is the force which does the self-work matching the radiated energy. One effect of this self-force is to extract or inject energy from the electrons depending on their longitudinal position—this dependence gets superimposed on the pre-existing energy "chirp". Because of local dispersion at the point of emission, this change of energy is immediately reflected in a changed horizontal betatron amplitude, and therefore a changed horizontal emittance.

A defect that is probably common to all measurements and simulations is the R_{56}-dependent emittance growth caused by bunch-charge-independent, nonlinear lattice forces. Unless eliminated, this mechanism can cause spurious emittance growth. The data analysis scheme used in the present report tries to compensate for this effect.

Part of present-day intense-electron-bunch lore is that CSR is the *only* source of emittance growth of an electron bunch in a magnetic field. One implication of this prejudice is that the emittance dilution should be insensitive to the transverse bunch dimensions. The lower right corner value of Table 1 seems to disagree with this contention. However, the emittance increase in this case is ascribable mainly to a "halo" observed in the simulation which seems to be an artifact of the numerical simulation, caused by the granularity of the beam representation. If the electron beam were, in fact, granular on the same scale as the simulation (that is, on a scale of roughly the bunch dimensions divided by 10) then a halo much like that in the simulation could be produced. In any case, since this emittance increase is due to only a small fraction of the particles, this would not represent growth of the core of the beam. The luminosity (in the case of colliding linacs) or the brilliance (in the case of x-ray sources) would therefore not be much affected by such a halo.

Based on the present simulation, for the standard chicane at high energy such as 5 GeV, the nonlinear effects just mentioned seem to have only small effects on transverse emittance growth compared to the CSR effect.

7.3. Speculations Concerning Halo Generation. The Touschek effect, analysed, for example, by Piwinski[**24**], is a well known phenomenon that is important for GeV-scale dense electron bunches. The Touschek lifetime in storage rings is typically of order an hour in storage rings. This suggests the effect will be negligible in a bunch compressor, but there are factors which may modify this. For one thing, the "healing" time constant for an electron suffering an encounter not quite close enough to be ejected from the storage ring is of order milliseconds rather than hours. The definition of what constitutes "halo" will therefore be very different for bunch compressors than it is for the Tousckek effect. A typical fractional momentum loss leading to particle loss in a storage ring might be $\Delta\delta_{\rm typ}^{\rm Touschek} \approx 10^{-2}$. A significant fractional momentum change in the bunch compressor compressor might be

$$\Delta\delta_{\rm signif.}^{\rm compressor} \approx \sqrt{\frac{\gamma\epsilon_x}{\gamma}\,\frac{\beta_x}{D^2}} \approx 10^{-4}. \tag{4}$$

Also, though the bunch compressor charge per bunch may not be large by storage ring standards, the bunch volume may be smaller by a factor of order 10^4. As it happens, Piwinski's formulas for the Touschek effect are not immediately applicable. The compressor set-up depends on the correlation between momentum and longitudinal position. As the bunch approaches the end of the chicane the head and tale approach each other transversely (in the bunch's frame) as they come into coincidence longitudinally. This configuration greatly enhances the Touschek-like scattering rate. Though Piwinski's treatment assumes no such correlation, his formulation is sufficiently general to make the inclusion seem straight forward.

Rough evaluations of Piwinski's formulas suggest that, in spite of all these factors, because the operative time is so short, single close encounter electron-electron scatters will still contribute negligibly to emittance growth within the compressor, (The same would not be true for the same bunches circulating in a ring.) This means that it is more appropriate to calculate true Touschek halo generation analytically rather than by numerical particle tracking simulation. In the present string space charge simulation a certain amount of halo generation has certainly been observed; for example a halo of a few particles can be seen in Fig. 6. But to extract meaningful halo production rate for electrons (as contrasted with macroparticles) from the numerical simulation will require a stochastic analysis far more sophisticated than we have at present.

In the present simulation with, say 1000 macroparticles, each macroparticle has effective transverse size equal to about one tenth of the smaller transverse bunch dimension. Bunch substructure on this scale, for example because of gun cathode nonuniformity, may occur in practice. The simulation suggests that bunch substructure on this (or shorter) scale is likely to lead to substantial halo production.

It has been noted previously that the longitudinal parameters (mean and r.m.s. energy loss) calculated in our simulation agree well with other calculations. The horizontal emittance growth for the round beam also agrees but, referring to Table 1, it can be seen that an appreciable fraction of its emittance growth is what we are now ascribing to halo. The emittance growth of the core predicted by our simulation is noticeably *less than* the other growth predictions. [8] These points may be mainly of academic interest since, for predicting the performance for future facilities, the emittance growth of the core is relatively small, even in the ribbon beam case.

There is one way in which the numerical simulation can be expected to give a faithful representation of halo behavior for real electron beams. It concerns the

[8] Incidentally, it is important to realize, referring to Eq. (5) that, unlike the treatment of string length, which is analytically exact (though dependent on the empirical string length) the treatment of string height is quite crude. In fact the treatment intentionally underestimates the impact of close-encounter impulses.

round/ribbon beam comparison. Once a prescription has been established for segregating halo from core, it seems that the contribution of halo to emittance should vary inversely with the bunch height, irrespective of whether real electrons or macroparticles are at issue. This inverse scaling behavior is what is observed for macroparticles in the simulation. Accepting that the round/ribbon ratio is the same for electrons and macroparticles has gone into establishing the lower right hand entry of Table 1.

It has by now been explained how an increase of horizontal emittance in the simulation can be due to the halo, not the core, of the distribution. (The angular single-scattering distribution falls off so slowly that a relatively small number of particles contribute disproportionally to the emittance.) Even in the extreme, ribbon-beam case, at the cost of increased computation time, this artifact could be suppressed by reducing the product of macroparticle charge and finite element interval.

The present simulation has suggested that halo generation may be significant in facilities employing bunch compressors, even at quite high beam energy. But, having emasculated all close encounters, the numerical, particle-by-particle, intra-beam scattering approach cannot reliably simulate Touschek-like halo generation directly. The code could, however, be adapted to perform Monte Carlo integrations of Piwinski's analytical formulas, for distributions more realistic than Piwinski's Gaussian distributions.

This report has profited greatly from the careful reading of earlier versions and detailed comments made by Lars Groening and by Frank Stulle.

8. Appendix: Implementation Details

Concerning the *physics* of the string space charge simulation, there have been three alterations of the code (primarily influencing transverse rather than longitudinal evolution) compared to the descriptions in the references given above:

- (To speed up the code) the forces in field-free regions are calculated analytically, using the (once-integrated) Heaviside-Poincaré-Schott formula[**3**] for the forces between parallel-traveling particles.
- For purposes of calculating the force field produced by a string, the string is also assigned a vertical height $2y_0$. By choosing this height small compared to the bunch height (typically $y_0 \approx \sigma_y/10$), the possibility of horizontal emittance growth due to vertical bunch nonuniformity is preserved. At the same time, even the only-logarithmically-divergent but unphysically-large (because of amplification proportional to macrobunch charge) deflections occurring in the occasional close encounter of microbunches, are eliminated. In the original paper closed form analytical formulas are given for the fields due to such extended sheets. But those formulas are very complicated and, in the UAl code, the effect of vertical string extension is modeled more crudely, but far more simply. The formulas for each of the force components acting on one string due to another are proportional to factors of the form $(a^2)^{-3/2}$, where a is approximately the separation distance of the source string and the string being tracked.) In a typical simulation the inequality $y_0^2 << a^2$ is respected for all but a few (extremely close) encounters. Assigning vertical height to one of the strings amounts making the replacement of this factor by its average

value:

$$\frac{1}{(a^2)^{3/2}} \rightarrow \Big\langle \frac{1}{\tilde{y}^2 + (a^2)^{3/2}} \Big\rangle = \frac{1}{y_0} \int_0^{y_0} \frac{d\tilde{y}}{(\tilde{y}^2 + a^2)^{3/2}} = \frac{1}{a_0^2} \frac{1}{y_0^2 + (a^2)^{1/2}}$$
$$< \frac{1}{(y_0^2 + a^2)^{3/2}}. \tag{5}$$

In the UAL code the initial expression in this chain of equalities and inequalities is simply replaced by the final expression. Apart from this change, all other string-model formulas are unchanged. This amounts to replacing the string by a vertical ribbon. For the vast majority of string encounters this replacement has negligible effect, but the transverse impulse suffered in the occasional close encounter is limited. Furthermore, the longitudinal impulses should not be much affected, since they are known to be insensitive to transverse position. For the occasional close encounter, instead of potentially being uncontrollably large, the transverse deflection is limited. This procedure does, however, bring in another *ad hoc* parameter $strH$, whose effect needs to be investigated in the simulation.

The sickness that is moderated by this trick has to do with occasional "halo particle" produced in close encounters. By varying $strH$ one can investigate the prevalence and importance of the halo particles.

- For the relatively small number of macroparticles for which the string space charge simulation is practical, there is another source of fluctuating dependence on Monte Carlo seed. Since emittance growth is a kind of diffusion, it can be expected to be most important in regions where the distribution functions are changing most rapidly. Distributions of a small number of macroparticles are sure to be "lumpier" than the distributions of the vastly more numerous true particles. In an attempt to cancel low order moments of the distributions, the UAL software allows the distributions to be "symmetrized". For example a distribution of 800 particles is generated by first choosing 400 particles into nominally-correct distributions and then completing the distribution with the same particles, but with their transverse phase space coordinates reversed. This trick seems to reduce fluctuations noticeably.
- As has been explained previously the maximum possible impulse imparted to a macroparticle is proportional to both the macroparticle charge and to the interval being represented numerically. Because the computation time scales only linearly with the bend splitting factor *nsplit*, but quadratically with number of macroparticles *np*, it is useful for the UAL code to support bend splitting in its string space charge code without the need for generating a separate input lattice description for each value of *nsplit*. For different reasons (the faithful treatment of the lattice optics) it is appropriate to similarly split quadrupoles into multiple segments. But the space charge effects in quadrupoles are quite unimportant, so the quadrupole splitting is ignored for space charge calculations. Bends are opposite—their splitting has little effect on the optics, but affects space charge. For these reasons, the UAL code supports the splitting of sbend elements for purposes of space charge calculations. (Of course such splitting can always be done in the external lattice file but the UAL code permits this to be done under the control of the "`.apdf`" file.)

The *computer engineering* updating of the code has been substantial. The actual source code can be viewed at reference[**16**]. To incorporate space charge the pre-existing UAL environment needed to be augmented by only a few classes, all shown in the following "`.apdf`" (accelerator propagator description format) file:

```
<apdf>
   <propagator id="stringsc" accelerator="ring">
      <create>
         <link algorithm="TEAPOT::DriftStringSCKick" types="Default" />
         <link algorithm="TEAPOT::DriftTracker" types="Marker" />
         <link algorithm="TEAPOT::DriftStringSCKick" types="Drift" />
         <link algorithm="TEAPOT::DipoleStringSCKick" types="Sbend" />
         <link algorithm="TEAPOT::MltStringSCKick"
                  types="Quadrupole|Sextupole|Multipole|[VH]kicker"/>
         <link algorithm="TEAPOT::RFCavityTracker" types="RfCavity"/>
         <link algorithm="TEAPOT::MltTracker" types="Kicker"/>
      </create>
   </propagator>
</apdf>
```

This file implements the UAL architectural principal according to which the lattice description file contains absolutely no specification as to what algorithms are to be employed in evolving particle or bunch properties through the lattice. The linkages of algorithms to lattice element types are completely specified in this "`.apdf`" file. (More complicated linkages, such as different algorithms for differently-named elements of the same type, are also possible, but are not needed here.) Simply by changing the algorithm linkages the space charge tracking can be turned on or off. All parameters governing the space charge are given on the command line (or, somewhat less conveniently, in the program itself) of the "`main.cc`" program, which provides the UAL "command language" mechanism.

The lattice itself (with all its parameters) is described in the so-called "`.sxf`" (standard exchange format) file. This file is most easily (and completely mechanically) produced as a fully-instantiated output from MAD-X[**15**], starting from a standard MAD input lattice description.

All results in this paper have been obtained using one laptop computer with N_p, the number of particles tracked, being of order one thousand (in most cases $N_p = 800$). Such a small number of particles might be expected to cause unacceptably noisy results. In fact the various plots in this paper are relatively smooth.

For greater reliability, one would prefer to track perhaps ten times as many particles. With the computation time scaling as N_p^2, this would make the computation unacceptably slow. One contemplates, therefore, using parallel processing to reduce the computation time by a factor almost proportional to the number of parallel computers, N_c, especially if one wishes to track bunches for one or more full turns around a circular ring.

For the string space charge method the computation time is dominated by the N_p^2 calculations of the space charge force on every particle by every other particle. Propagating the particles from one space charge kick location to the next is relatively quick. A natural division of the labor is to divide the N_p particles into groups each containing N_p/N_c particles, with one group allotted to each computer, which calculates all space charge deflections for its own group of particles, and propagates them to the next space charge location. The parallelization overhead comes from broadcasting all $6N_p$ particle coordinates to all N_c computers each time a space charge kick location is encountered. (At the moment the code uses only the three position coordinates, but an eventually more accurate calculation would depend also on the slope coordinates.)

Bibliography

[1] R. Talman, *String Formulation of Space Charge Forces in a Deflecting Bunch,* PRST-AB, **7**, 100701, 2004

[2] N.Malitsky and R.Talman, *UAL Implementation of String Space Charge Formalism,* WE-PLT154, EPAC Conference, Lucerne, Switzerland, 2004

[3] R.Talman, *Accelerator X-Ray Sources,* all of Chap. 13, Wiley-VCH, Weinheim, 2006

[4] A. Kabel et al., *Using TraFiC4* to Calculate and Minimize Emittance Growth Due to CSR,* Nucl. Instrum. & Metods, A **455**, 185, (2000)

[5] M. Borland, ELEGANT*: A Flexible SDDS-Compliant Code for Accelerator Simulation,* LS-287, Argonne National Laboratory, 2000

[6] R.Talman, *Novel Relativistic Effect Important in Accelerators,* PRL **56**, 1429

[7] H. Braun, *Experimental Results and Technical Results and Developments at CTFII*, CERN/PS 2000-030 (AE), CLIC-Note 441, 2000

[8] H. Braun et al, *Emittance Growth During Bunch Compression in the CTF-II*, Phys. Rev. Lett., **84** 658, 2000

[9] H. Braun et al, *Emittance Growth and Energy Loss Due to Coherent Synchrotron Radiation in a Bunch Compressor*, PRST-AB, **3**, 124402, 2000

[10] M. Chanudet-Cayla, *Simulations of Beam Dynamics in the CTF2 Drive Beam Accelerator and Bunch Compression*, CLIC Note 429, PS/RF Note 2000-006, 2000

[11] L. Groening et al., *Recent Experiments on the Effect of Coherent Synchrotron Radiation on the Electron Beam of CTF II*, `http://groening.home.cern/groening/csr_00.htm`, PAC 2001

[12] H.H. Braun et al., Recent Experiments on the Effect of Coherent Synchrotron Radiation on the Electron Beam of the CTF II, IEEE, Proceedings of the 2001 Particle Accelerator Conference, Chicago, p. 164

[13] *Coherent Synchrotron Radiation,* CSR Workshop, Berlin 2002, `http://www.desy.de/csr`

[14] P. Emma, *CSR Benchmark Test-Case Results,* CSR Workshop, Berlin 2002

[15] MAD-X website `http://mad.web.cern.ch/mad/`

[16] UAL website `http://www.agsrhichome.bnl.gov/UAL/`

[17] L. Giannessi, *Simulation codes for high brightness electron beam free-electron laser experiments,* PRST/AB, **6**, 114802 (2003)

[18] F. Stulle et al., *Designing a bunch compressor chicane for a Multi-TeV linear collider,* PRST/AB **10**, 031001 (2007)

[19] Ya.S. Derbenev, et al., *Microbunch Radiative Tail-Head Interaction,* TESLA-FEL, 95-05, 1995

[20] B,E. Carlsten and T.O. Raubenheimer, *Emittance growth of bunched beams in bends*, Phys. Rev. E, **51**, 2, 1435 (1995)

[21] J. Schwinger, *On Radiation by Electrons in a Betatron*, unpublished notes, 1945, transcribed by Miguel Furman, LBNL-39088/CBP Note 179, 1996

[22] M. Bassetti, *Analytical Formula for the Centrifugal Space Charge Effect,* CERN/LEP-TH/86-13, 1986

[23] M. Bassetti and D. Brandt, *Transverse Electromagnetic Forces in Circular Trajectory,* CERN/LEP-TH/86-04, 1986

[24] A. Piwinski, *The Touschek Effect in Strong Focusing Storage Rings,* ISSN 0418-9833, DESY Report 98-179, 1998